



BNL-112739-2016-JA

Devices for SRF material characterization

P. Gouket, T. Junginger, B. P. Xiao

Submitted to Superconducting Science and Technology

October 2016

Collider-Accelerator Department

Brookhaven National Laboratory

**U.S. Department of Energy
Office of Science,
Office of Nuclear Physics**

Notice: This manuscript has been co-authored by employees of Brookhaven Science Associates, LLC under Contract No. DE-SC0012704 with the U.S. Department of Energy. The publisher by accepting the manuscript for publication acknowledges that the United States Government retains a non-exclusive, paid-up, irrevocable, world-wide license to publish or reproduce the published form of this manuscript, or allow others to do so, for United States Government purposes.

DISCLAIMER

This report was prepared as an account of work sponsored by an agency of the United States Government. Neither the United States Government nor any agency thereof, nor any of their employees, nor any of their contractors, subcontractors, or their employees, makes any warranty, express or implied, or assumes any legal liability or responsibility for the accuracy, completeness, or any third party's use or the results of such use of any information, apparatus, product, or process disclosed, or represents that its use would not infringe privately owned rights. Reference herein to any specific commercial product, process, or service by trade name, trademark, manufacturer, or otherwise, does not necessarily constitute or imply its endorsement, recommendation, or favoring by the United States Government or any agency thereof or its contractors or subcontractors. The views and opinions of authors expressed herein do not necessarily state or reflect those of the United States Government or any agency thereof.

Devices for SRF material characterization

P. Goudket^{1,2}, T. Junginger^{3,4}, B.P. Xiao⁵

¹ASTeC, STFC Daresbury Laboratory, Warrington, Cheshire WA4 4AD, UK

²Cockcroft Institute, Warrington, Cheshire, UK

³TRIUMF Canada's National Laboratory for Particle and Nuclear Physics

⁴Helmholtz-Zentrum Berlin fuer Materialien und Energie (HZB), Germany

⁵Collider Accelerator Department, Brookhaven National Laboratory, Upton, NY, U.S.A.

E-mails: philippe.goudket@stfc.ac.uk, tobi@triumf.ca, binping@bnl.gov

The surface resistance R_s of superconducting materials can be obtained by measuring the quality factor of an elliptical cavity excited in a transverse magnetic mode (TM_{010}). The value obtained has however to be taken as averaged over the whole surface. A more convenient way to obtain R_s , especially of materials which are not yet technologically ready for cavity production, is to measure small samples instead. These can be easily manufactured at low cost, duplicated and placed in film deposition and surface analytical tools. A commonly used design for a device to measure R_s consists of a cylindrical cavity excited in a transverse electric (TE_{110}) mode with the sample under test serving as one replaceable endplate. Such a cavity has two drawbacks. For reasonably small samples the resonant frequency will be larger than frequencies of interest concerning SRF application and it requires a reference sample of known R_s . In this article we review several devices which have been designed to overcome these limitations, reaching sub - $n\Omega$ resolution in some cases. Some of these devices also comprise a parameter space in frequency and temperature which is inaccessible to standard cavity tests, making them ideal tools to test theoretical surface resistance models.

1. Introduction

1.1. The need for RF sample testing of materials for superconducting cavities

In particle accelerators superconducting RF (SRF) cavities are generally used to take advantage of the extremely low surface resistance provided by the superconductor and thereby minimize losses in the cavity walls. This is particularly interesting when high duty cycle or even continuous wave (CW) operation is required.

The material of choice for SRF cavities is niobium, as it has the highest single-element critical temperature and lower critical field H_{c1} [1] as well as good mechanical and thermal properties. Niobium cavities are generally made of bulk material, though some of the earliest cavities were Nb-coated copper cavities used for the LEP [2] taking advantage of the higher thermal conductivity of copper. This approach also has the advantage of the lower price of copper compared to niobium. Niobium-on-copper cavities have a lower surface resistance at 4.2 K (at low gradient levels) and do not require shielding from the Earth's magnetic field. Currently this approach is used for cavities in the LHC and HIE-Isolde at CERN and ALPI at INFN Legnaro. Current performance levels of niobium-coated copper structures are inferior to those of bulk niobium technology, as their surface resistance increases strongly with field. New deposition techniques are being developed to overcome current limitations. Some of them are not on a technological readiness level

42 for deposition on a cavity and therefore require testing of small samples to probe their RF performance and
43 streamline optimization of the coating process.

44 Theoretically the maximal field achievable under RF is defined by the superheating field H_{sh} of the
45 cavity material. For the case of niobium, a type-II superconductor, this is about 240 mT (at 0 K), which
46 corresponds to an accelerating gradient of 57 MV/m [3] for the widely used TESLA shaped cavity. In
47 practice after years of development and optimization of cavity shapes, manufacture and processing tech-
48 niques accelerating gradients in excess of 50 MV/m [4] and Q-values close to the theoretical limit are
49 achieved in single-cell Nb cavities at frequencies of 1.3 GHz. Bulk niobium technology is thus approaching
50 its fundamental limitations. Optimization of the cavity shape can push the maximum Q-value and acceler-
51 ating gradient by some percent but to achieve a performance significantly exceeding the state of the art one
52 has to change to materials other than bulk niobium. Therefore there is an active field of research into new
53 materials potentially displaying higher performance than niobium, such as NbN, NbTiN, MgB₂ and Nb₃Sn
54 [5]. Of these materials only Nb₃Sn has been successfully deposited on an SRF cavity and shown to have a
55 performance exceeding bulk niobium at least at 4.2 K for a moderate accelerating gradient [6]. To assess
56 the RF performance of other new materials and optimize coating procedures the community currently has
57 to rely on sample tests.

58 As mentioned above best performance of materials other than niobium has been achieved with Nb₃Sn.
59 Results however suggest that this material is currently limited by vortex penetration at fields at defects far
60 below its superheating field [7]. Strong dissipation from vortex penetration could possibly be avoided by
61 depositing nanometer-thin multilayers of superconductors and insulators on a niobium cavity, as suggested
62 in 2006 by A. Gurevich [8]. So far only small samples have been produced since this complex technology
63 is not yet ready for depositing films on full scale cavities. Therefore, this is another process whose optimi-
64 zation depends on the testing of small samples.

65 The operational limitations of elliptical SRF bulk niobium cavities have been pushed back over the
66 many years of research since their first use. We are now approaching the fundamental limits of this material.
67 However, neither cavities of different shape, such as quarter wave resonators, nor cavities of different ma-
68 terials such as Nb₃Sn are performing close to their fundamental limits. While the ideal approach to test new
69 materials for SRF applications is to produce cavities as used in the particle accelerators, this approach is
70 costly and some materials are not yet developed enough and require testing of small samples.

71 This article focuses on devices which allow measuring the surface resistance of samples. Before per-
72 forming these tests samples can be characterized by several DC methods. These include RRR measurements
73 [9] which give information on the sample purity and electron mean free path, and AC susceptibility meas-
74 urements [10] which are typically performed at 100 Hz -10 kHz and can give information on flux dynamics.
75 DC SQUID magnetic susceptibility measurements [11] allow one to gain information on the magnetization
76 curve of the sample. Attempts have been made to extract the H_{c1} and H_{c2} from this curve, but this requires
77 complex sample alignment and interpretation of the results is still controversial. Also possible are field
78 penetration measurements, which is a technique dating from the 1930s but only recently used for thin film
79 measurements [12]. Several other material and surface analytic techniques have been applied to SRF cavity
80 materials. An overview can be found in reference [13]. All these DC methods can be useful to characterize
81 the film quality and can guide coating parameter optimization. They fail however to predict the RF perfor-
82 mance of the samples. It is thus required to test these samples under RF exposure to relate the surface
83 properties to the RF performance.

84 While this article focuses on devices which allow measuring the surface resistance of samples, other
85 methods to characterize RF losses exist and are being briefly reviewed in the following section.

86 1.2 Other methods to measure losses of superconductors under RF

87

88 The sample test cavities which will be reviewed in the following chapter all allow the measurement of the
89 surface resistance of an attached sample. Other options to explore the loss mechanisms of superconductors
90 under RF exposure are beyond the scope of this article. However in this section some alternative approaches
91 will be briefly mentioned. The most straightforward option is to use single-cell cavities and measure their
92 quality factor. The surface resistance derived from this measurement has then to be taken as averaged over
93 the whole surface area. To gain information about the distribution of the losses on the sample surface several
94 temperature sensors can be placed on the cavity's outer surface. This widely used technique is called tem-
95 perature mapping or simply T-mapping [3]. In order to gain direct information about the temperature dis-
96 tribution on the inner cavity surface JLab has developed a laser beam scanning apparatus [14]. This laser
97 beam not only allows measurement of the surface temperature but can also be used to move vortex hot
98 spots. Pushing them to lower field regions can significantly decrease the overall losses [15].

99 Most single cell cavity tests have been performed on 1.3 or 1.5 GHz cavities, which are large compared
100 to typical sample sizes of the devices focused on in this article. INFN Legnaro has developed an infrastruc-
101 ture to test significantly smaller 6 GHz cavities allowing for quick turnarounds, since these cavities can be
102 directly inserted into a liquid helium dewar [16]. A helium transfer from a dewar to a test cryostat is thus
103 not required. Evidence for thermal boundary resistance effects on the surface resistance of niobium cavities
104 was found [17].

105 Most surface resistance studies have been performed on elliptical cavities. An open question in SRF is
106 why cavities of different geometries like quarter or half wave cavities generally exhibit a stronger decrease
107 of the quality factor Q_0 with applied field strength. TRIUMF is currently developing coaxial resonators
108 which can be heat treated in an induction furnace to explore this in detail [18].

109 All devices presented in this article are designed to measure the surface resistance of samples with
110 diameters of typically a few cm. University of Maryland scientists have developed a system to measure
111 third harmonics nonlinearities of superconductors in the sub-micrometer scale using a magnetic write head.
112 Niobium and MgB_2 have been investigated. The nonlinear response was found to be localized in niobium
113 and uniform in MgB_2 [19].

114 2. Measurement techniques

115
116 In order to measure the surface impedance of a sample surface, it is necessary to make the sample a part of
117 a resonant structure. Such a sample could be a rod [20, 21], a flat disc [20, 22-34] or just a small piece [20,
118 35, 36] inserted into the cavity inner surface. The cavity is then excited in a particular mode with the reso-
119 nant frequency and Q_0 easily measurable, allowing one to calculate the surface impedance in a straightfor-
120 ward way [20, 22, 23, 25-30, 37, 38] based on average losses and differential measurements with calibrated
121 samples. Another way to measure the surface impedance with significantly higher resolution is to use a
122 power compensation technique that combines calorimetric measurements with RF measurements [24, 31-
123 36].

124 2.1. Choice of cavity geometry

125
126 Cylindrically symmetric cavities operating in a TE_{0xx} mode are commonly chosen as the resonant circuits
127 [20, 21, 23, 25, 28-34, 37, 38]. In such a cavity with these modes the electric field lines are simple self-
128 closing rings around the resonator axis and electric field lines vanish on cavity walls as well as on the
129 sample, if positioned at the lateral end of the cavity. Moreover, in the ideal geometry, no RF current crosses
130 the joint between the sample and the cavity and, with no electric fields normal to the cavity surface, elec-
131 tronic problems such as multipacting and heating due to dark current may be avoided.

132 For simple cavity geometries, these TE_{0xx} cavities can only be used to measure large-sized samples while
133 maintaining suitably low resonance frequencies.
134

135 Other attempts with more complicated geometries, including the “triaxial” cavity [24], “quadrupole
 136 mode resonator” [35, 36], “mushroom cavity” [26, 27] and sapphire loaded Surface Impedance Character-
 137 ization (SIC) cavity [31-34] have been made, trying to overcome the limitation of simple TE mode cavities.

138 2.2. Choice of measuring technique

139 A simple way to measure the surface resistance is to measure the quality factor Q_0 change with a reference
 140 sample and the sample to be measured, so called end-plate replacement technique, which is used since more
 141 than 40 years [39]. It requires a reference sample. The reference sample is usually surface treated using the
 142 same way of the cavity, so that the surface resistance of the cavity and the sample are the same. Using a
 143 copper cavity as an example, we assume the quality factor of the cavity with reference sample Q_1 at 2×10^5 ,
 144 geometry factor G at 300, filling factor of the sample η (the loss on the reference sample versus the total
 145 loss) at 40%, and the sample’s surface resistance R_s is much smaller than the surface resistance of copper.
 146 Then Q_2 , the quality factor of the cavity with sample to be measured, should be 5×10^5 . R_s can be calculated
 147 using
 148

$$149 R_s = \frac{G}{\eta} \left(\frac{1}{Q_2} - \frac{1}{Q_1} \right) + \frac{G}{Q_1} \quad (1)$$

150 Typically, the quality factor measurement error will be about 5%, from equation (2)

$$151 \Delta R_s = \sqrt{\left(\frac{G \Delta Q_2}{\eta Q_2^2} \right)^2 + \left[G \left(1 - \frac{1}{\eta} \right) \frac{\Delta Q_1}{Q_1^2} \right]^2} \quad (2)$$

152 one can get that ΔR_s should be 0.14 m Ω . In this case quality factor measurement with a copper cavity is
 153 not preferred for SRF samples. In a case where a niobium cavity with a Q_1 at 2×10^9 was used, ΔR_s would
 154 be improved to 14 n Ω . Despite its lower resolution compared to the other techniques introduced below, this
 155 approach is still used, since it allows for designing simple systems and performing quick tests.

156 Another way to measure the surface resistance with a significantly higher resolution is a power com-
 157 pensation technique, which allows the derivation of the surface resistance from a DC measurement. In a
 158 calorimetric system the sample and the host cavity are thermally decoupled. A DC heater (resistor) and
 159 at least one temperature sensor is attached to the back side of the sample. This allows for independent control
 160 of the sample temperature.
 161

162 A calorimetric measurement consists of two steps, see Figure 1:

163 1. The temperature of interest is set by applying a current to the resistor on the back side of the sample.
 164 The power dissipated P_{DC1} is derived from measuring the voltage across the resistor.

165 2. The RF is switched on and the current applied to the resistor is lowered to keep the sample tempera-
 166 ture and the total power dissipated constant.

167 The RF power dissipated in the sample, P_{RF} , is the difference between the DC power applied without
 168 RF, P_{DC1} , and the DC power applied with RF, P_{DC2} . P_{RF} is directly related to the surface resistance of the
 169 sample R_s and the magnetic field on the sample surface B ,

$$170 P_{RF} = P_{DC1} - P_{DC2} = \frac{1}{2\mu_0^2} \int_{Sample} R_s(B) |\vec{B}|^2 dS \quad (3)$$

171 Assuming R_s to be constant over the sample surface area and independent of B , the above equation
 172 simplifies to:

$$173 P_{RF} = P_{DC1} - P_{DC2} = \frac{R_s}{2\mu_0^2} \int_{Sample} |\vec{B}|^2 dS \quad (4)$$

174 which can be rearranged to yield an expression for the surface resistance:

$$175 R_s = \frac{2\mu_0^2 (P_{DC1} - P_{DC2})}{\int_{Sample} |\vec{B}|^2 dS} \quad (5)$$

176 An electromagnetic simulation and an RF calibration is needed to relate $|B|^2 dS$ to the transmitted power
 177 measured in the experiment. Details are described in references [33, 40].

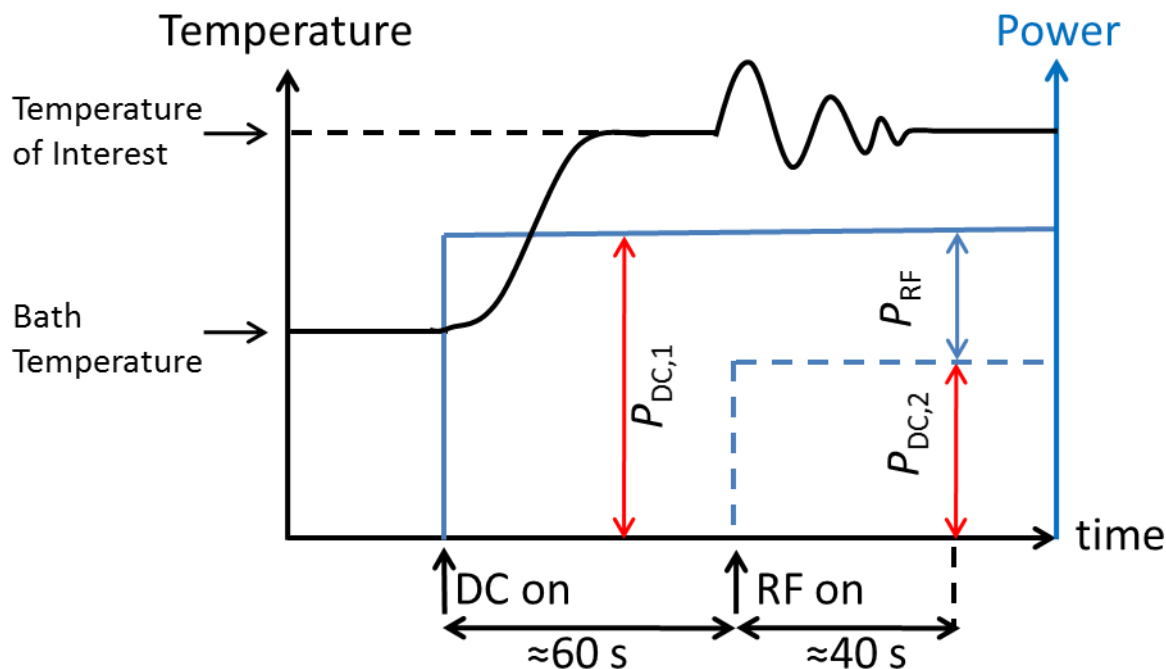


Figure 1: In a calorimetric system the surface resistance of a superconducting sample is derived from a DC measurement [40].

The calorimetric measurement gives a high resolution on the surface resistance measurement. The DC power is measured using a four-probe technique, and a high-precision current source and voltmeter. Temperature measurements give a resolution better than 5 mK. The magnetic field is calculated from RF power measurements and decay time measurement, with an accuracy better than 5%. The slow variation of helium bath pressure can be ignored since the data is taken within a few minutes. The ripple of the helium bath pressure, normally better than 100 μ bar, will give a 1 mK temperature fluctuation at 2 K bath temperature, which can already be better than the resolution of the thermal sensors. Finally the resolution of a calorimetric system will be limited by the minimal detectable heating and therefore depend on the resolution of the voltmeter and temperature readout. Thus the resolution can be obtained by differentiating equation (5) with respect to P_{DC2} yielding:

$$|\Delta R_s| = \frac{2\mu_0^2 \Delta P_{DC2}}{\int_{sample} |\vec{B}|^2 dS} \quad (6)$$

This equation directly shows why these systems have a much higher resolution for R_s for higher fields. The resolution of ΔR_s can be in sub- n Ω range since it is mainly limited by the DC power measurement.

The above two methods are not sufficient for investigating localized effects that will cause non-uniform temperature distribution on the sample. Temperature mapping system could be a supplemental system to investigate the non-uniform RF loss mechanism on the sample. In these systems, diodes, carbon Allen-Bradley thermal sensors, or CernoxTM thermal sensors will be mounted on the back of the sample (opposite to the surface that is exposed to the RF) near the high magnetic field region. A 4-wire setup is used to accurately measure the temperature with sub mK to 10 mK resolution. Apiezon[®] N grease is usually applied on top of each thermal sensor to ensure good thermal contact between cavity surface and sensor, together with the pressure provided by a spring loaded pin that will get compressed during the test.

3. An overview of devices

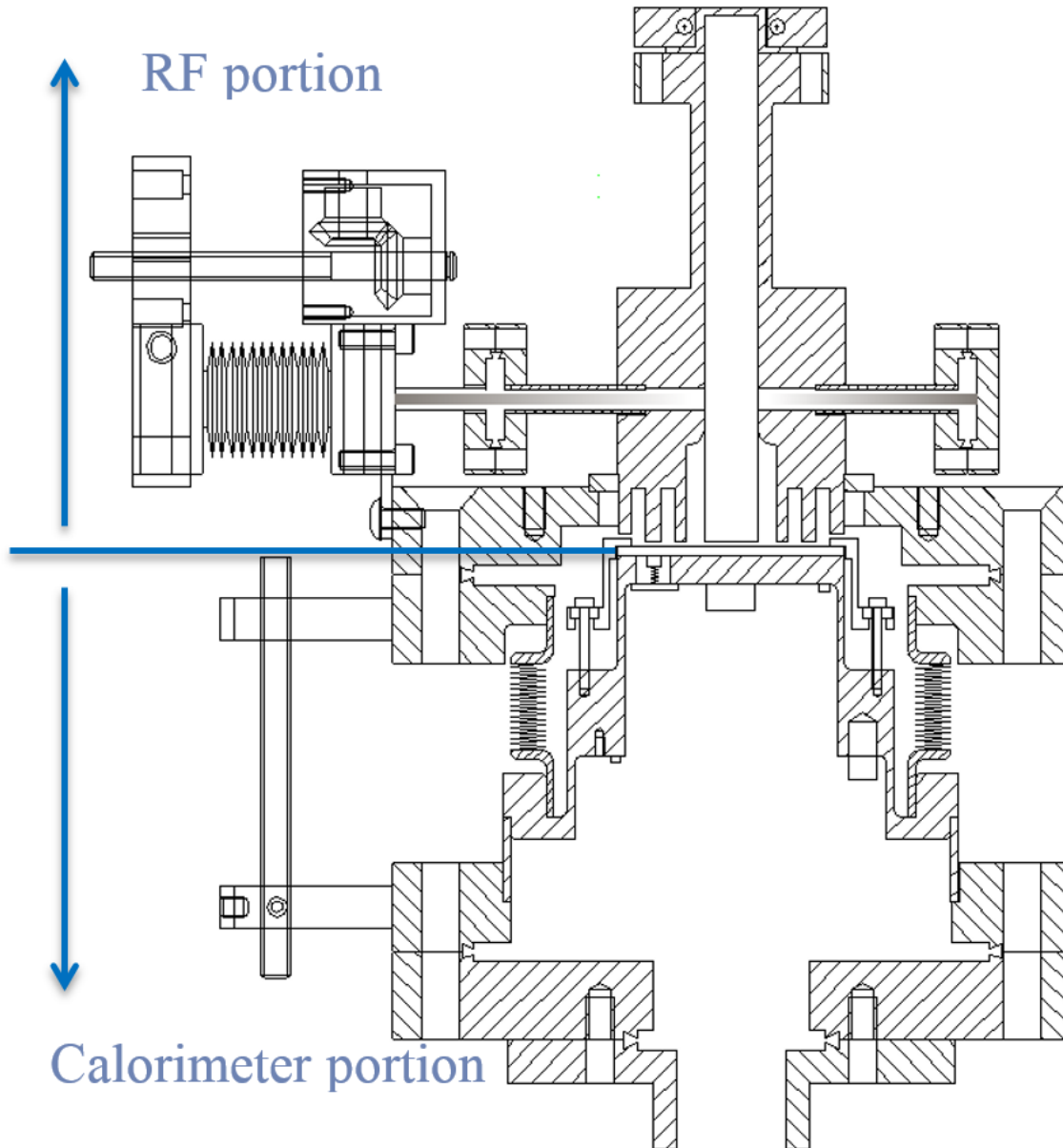
The early activities of developing devices for surface impedance measurement of SRF sample material can be traced back to the early 1970s. Bruynseraede et al. used a cylindrical TE_{011} cavity to measure the surface resistance of lead, indium and an indium-lead alloy by the sample replacement technique [39]. Different cavity shapes and measurement techniques were investigated in the 1980s. For example, Delayen et al. designed apparatuses to measure samples with different geometries, like rods, small samples and flat rounded samples [20]; Kneisel et al. designed a cylindrical TE_{011} Nb cavity to measure flat rounded samples [25], with a temperature mapping system on the bottom of the sample to resolve the spatial resistance difference; Klein et al. used a cylindrical TE_{011} Cu cavity to measure the surface resistance of YBCO [28] between 4 K and room temperature; Liang et al. designed a “triaxial” cavity to measure 1 inch diameter samples at 1.5 GHz below 25 mT [24]. In the new century these activities exploded all around the world, with a variety of RF designs to focus the magnetic field on the sample and trying to maintain low resonant frequencies while keeping the sample size small [26, 27, 30, 31, 33, 35, 40-44]. These activities become critical with the rapid developments on pushing the performance of bulk Nb cavity to its theoretical limitations [4, 45-47], as well as the theoretical and experimental breakthrough of thin films [6-8]. In this section we focus on devices which are currently used or under development. These are the SIC system from JLab, the quadrupole resonators from CERN and HZB, the mushroom cavities from three different labs, the cylindrical cavity from CEA Saclay and IPN Orsay, and the choked resonator under development at STFC Daresbury.

3.1. SIC

The SIC system is based on a cylindrical polycrystalline niobium cavity with 2 cm inner diameter, shown in Figure 2. A HEMEX[®] sapphire rod from Crystal Systems is inserted into the cavity to lower the resonant frequency from around 20 GHz (without sapphire) to 7.4 GHz in the TE_{011} mode. An adjustable loop input coupler is located above the cavity, and its external quality factor can be varied from 10^6 to 10^{10} for this mode. The sapphire is tightly held from the top, and its bottom surface is set to be coplanar with the bottom of the cavity. The sample is located at the open end of the cavity and is thermally isolated from the bottom plane of the cavity cylinder and sapphire, being separated from them by a 0.02 cm gap. Two RF choke joints with a 1 cm depth are used at the bottom of the cavity to minimize the RF power leakage. This system provides well-controlled RF fields within the central 0.8 cm^2 area of samples with 5 cm in diameter. Cylindrically symmetric cavity operating in a TE_{011} mode is chosen as the resonant circuit for the SIC RF system. In such a cavity with this mode, the electric field lines are simple self-closing rings around the resonator axis and electric field lines vanish on cavity walls as well as on the sample, if positioned at the lateral end of the cavity. Moreover, in the ideal geometry, no RF current crosses the joint between the sample and the cavity and, with no surface-normal electric fields, electronic problems such as multipacting and heating due to dark current may be avoided. Compared to other designs, the SIC system inherits the merits of TE structure cavities and offers a good solution to the size issue while keeping the resonant frequency relatively low. And the unique design of the SIC system guarantees controlled RF field within the center of the sample, which simplifies the sample and sample holder structure and ensures the success of the RF-calorimetric combination measurement. The sample edges and the joint between sample and sample holder are shielded from high RF fields, therefore anomalous heating from vortex entry at edges is avoided. The sample mounting system is designed to be able to quickly swap the sample and to adopt a variety of samples with different substrates. The SIC uses the high precision calorimetric measurement technique. In a typical measurement with more than 5 mT applied magnetic flux density, the resolution of R_s will be 1.1 n Ω at 2 K and 6.6 n Ω at 9

250 K. However the SIC system works at a frequency much higher than cavity operation frequency, which is
 251 normally at 1.3 or 1.5 GHz, and the highest achieved magnetic field is at 14 mT.

252 The SIC system is used to measure the R_s of a variety of samples. Besides bulk Nb and thin film Nb
 253 samples [32, 33, 48, 49], this system is also used to measure the alternative materials like MgB_2 [50],
 254 Nb_3Sn [51], NbN[52] and NbTiN[53], as well as different multilayer thin films: NbTiN-AlN-Nb, NbTiN-
 255 AlN-Nb- Al_2O_3 , NbN-MgO-Nb, MgB_2 -MgO-Nb-MgO[52, 53], and Nb_3Sn - Al_2O_3 -Nb[54]. At 7.5 GHz, the
 256 single crystal MgB_2 films on 5 cm diameter sapphire disks fabricated by a hybrid physical chemical vapor
 257 deposition (HPCVD) revealed a $9 \pm 2 \mu\Omega$ surface resistance at 2.2 K, and exhibited a lower surface re-
 258 sistance than Nb at temperatures above 4 K [50].



259 Figure 2: SIC system overview, the top part is the RF portion and the bottom part is the calorimeter portion,
 260 with two parts joined by the 5 cm diameter sample. The RF portion includes a sapphire-loaded cylindrical
 261

262 cavity with choke joints, one fixed pickup coupler and one tunable fundamental power coupler. The calo-
 263 rimeter portion includes a sample holder with sensors and heaters, and a thermal path to the helium bath.
 264 [33]

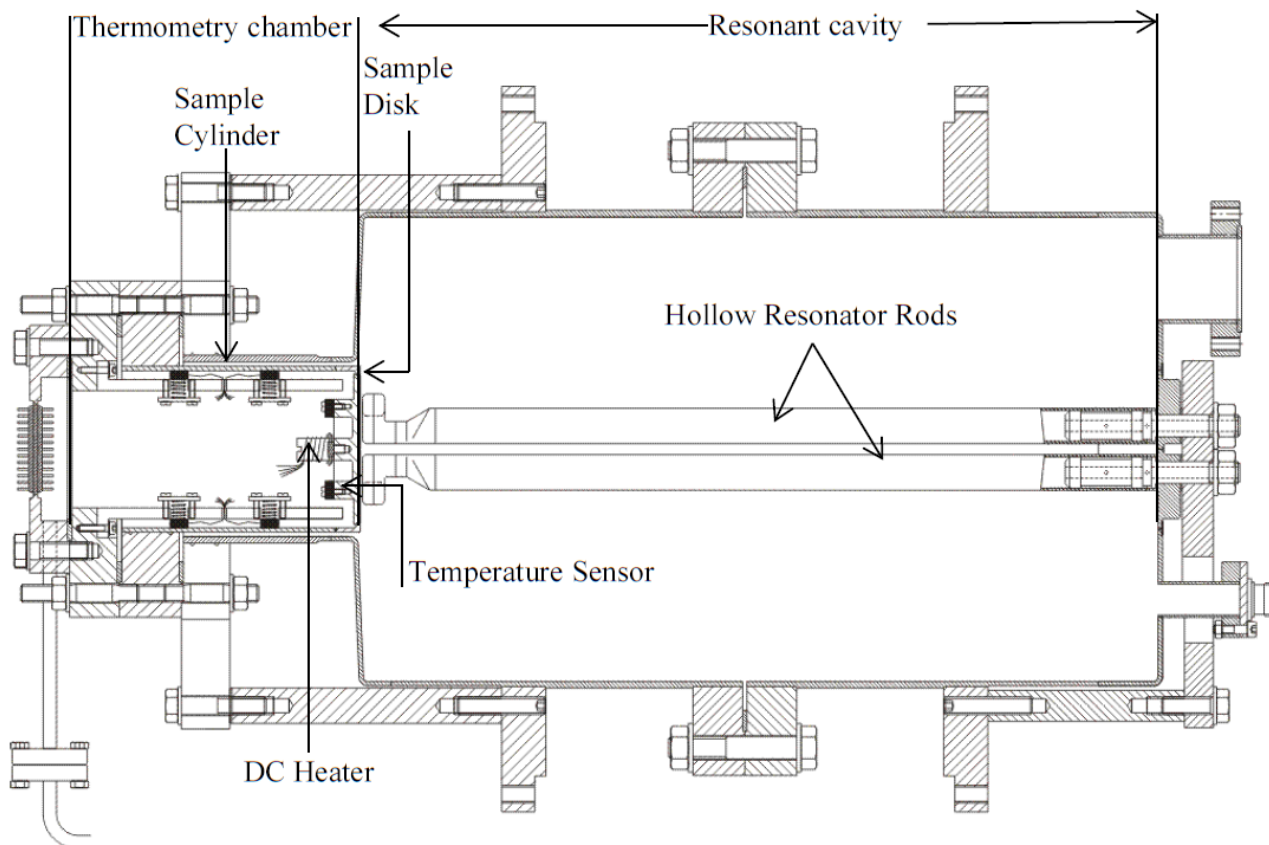
265

266 3.2. Quadrupole resonator

267

268 3.2.1. CERN Design

269 The quadrupole resonator shown in Figure is a four-wire transmission line half-wave resonator designed
 270 and built in 1997 for excitation in a TE_{210} -like mode at 400 MHz [35]. The magnetic field is at its maximum
 271 on the top plate where the resonator rods are attached to the host cavity on the crooked rods illuminating
 272 the sample surface at the bottom. The geometry also allows for excitation at multiple integers of 400 MHz
 273 (TE_{211} , TE_{212} -like...). In the case of the 800 MHz mode there is one additional peak along the rod, while in
 274 the case of the 1200 MHz mode there are two additional peaks along the rod. It has been commissioned for
 275 the frequencies of 400, 800 and 1200 MHz [55].



276

277 Figure 3: Quadrupole resonator: The sample disk is electron beam welded to the sample cylinder, which
 278 forms a coaxial structure with the host cavity. Inside of this narrow gap, the RF fields are exponentially
 279 decaying limiting the losses at the flange where the sample cylinder is mounted onto the host cavity. [35,
 280 55]

281

282 The quadrupole resonator consists of two 2 mm thick niobium cans for convenient handling and cleaning
 283 of the device, as shown in Figure . These cans are flanged to each other in the middle of the resonator,
 284 where the screening current on the cavity surface vanishes for the modes at 400 and 1200 MHz. For the 800

285 MHz mode the screening current has a maximum at this position. However, since the field is strongly con-
286 centrated around the rods in the middle of the resonator, excitation and measurements at 800 MHz are not
287 perturbed by losses at this flange. The quadrupole resonator is equipped with two identical strongly over-
288 coupled antennas. One serves as the input, the other as the output. Due to this configuration almost the
289 whole power transmitted to the cavity is coupled out and only about 1% is dissipated in the cavity walls
290 and on the sample surface. The system acts like a narrowband filter with minor losses.

291 The cover plate of a cylinder attached to the cavity in a coaxial structure serves as the sample, see
292 Figure 3. This design yields exponentially decaying RF fields between the outer wall of the sample cylinder
293 and the host cavity. Therefore, the power dissipated inside this 1 mm gap and at the end flange and joint of
294 the sample cylinder is negligible. A DC heater and several temperature sensors are attached to the back side
295 of the sample, which is thermally decoupled from the host cavity. As in the SIC the surface resistance of
296 the sample is measured by the calorimetric method explained in Section 2. The resolution in case of a
297 niobium sample for an applied field of 5 mT at 400 MHz is 0.44 n Ω at 2 K and 2.2 n Ω at 8 K limited by the
298 resolution of the temperature controller which is 0.1 mK. For higher magnetic field the resolution is better,
299 while for materials of higher thermal conductivity, in particular niobium films on copper substrate, it is
300 worse [40]. The maximum field obtained with the Quadrupole resonator is 70 mT at 400 MHz limited by a
301 quench of the cavity. This limit is reached independent of duty cycle suggesting that it is not a thermal
302 limitation.

303 One major difference between the Quadrupole Resonator and most similar devices is that the sample is
304 illuminated by RF magnetic and electric fields simultaneously like the surface in accelerating cavities.
305 While the magnetic field configuration is almost identical for the three used quadrupole modes, the ratio
306 between magnetic and electric field is different for each mode. It scales quadratically with frequency. This
307 follows directly from the law of induction for the quadrupole resonator geometry. This feature can be used
308 to distinguish between electric and magnetic losses. An upgrade of the system with a coil around the sample
309 cylinder enables testing the influence of flux trapping and cooldown speed on the surface resistance [40].

310 Measurements on a bulk niobium sample at three frequencies and several temperatures have shown that
311 the losses from thermally activated quasiparticles (from the so called BCS surface resistance) factorize in a
312 field and a frequency dependent part [40]. A comparison of a niobium film sample with a bulk niobium
313 sample of same residual resistance ratio (RRR) was performed. Comparing these results to the microstruc-
314 ture of Nb films suggest that a low crystal defect density and an excellent adhesion of the film on its sub-
315 strate are key aspects for niobium film cavities with a performance equal to bulk niobium technology [56].

318 3.2.2. HZB Quadrupole Resonator

319 Based on the CERN design a modified version of the Quadrupole Resonator has been developed [57]. The
320 design frequency has been shifted to multiple integers of 433 MHz in order to use existing RF equipment
321 optimized for 1.3 GHz. A number of relevant figures of merit have been improved to provide a higher
322 resolution, a lower peak electric field and less sensitivity to microphonics [57]. The new device has been
323 successfully commissioned and a peak magnetic field on the sample surface of 120 mT has been achieved
324 [43], which is almost twice as high as what has been possible using the CERN version. One drawback of
325 the Quadrupole Resonator is that the sample disk has to be electron beam welded to the sample cylinder.
326 Most thin film deposition devices are not suitable to accommodate the whole sample cylinder. Therefore it
327 is necessary to coat the sample disk first and weld it afterwards to the cylinder as has been done in [56].
328 This procedure carries the risk of a contamination after deposition. An alternative calorimetry chamber was
329 developed, providing samples of 12 mm height which are easily exchangeable. The parts are connected by

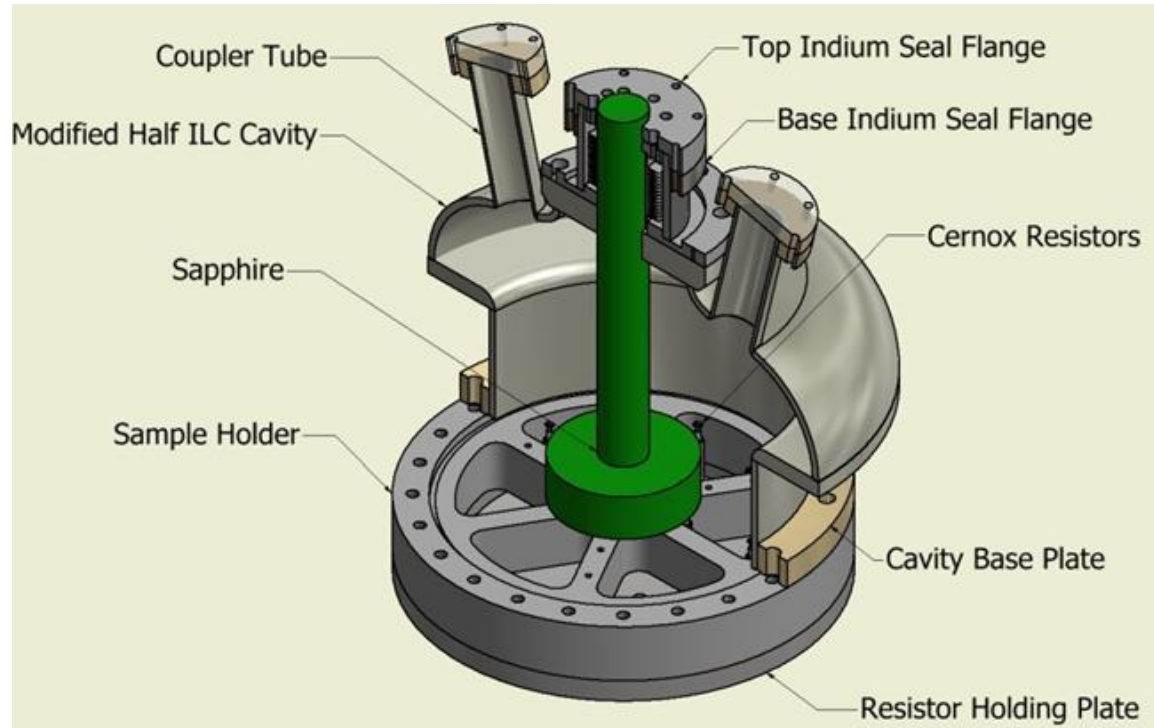
screwing connections and sealed using indium wire gaskets. Flexibility in mounting height and exchangeability of samples between the resonators at HZB and CERN are achieved by adapting individual bottom flanges [58].

3.3. Mushroom cavities

In a cylindrically symmetric cavity operating in a TE_{0xx} mode with a sample placed at one open end, a higher ratio of diameter/length is preferred to confine magnetic field on the sample. However, this setup will also produce high magnetic field at the end opposite to the sample. By deforming the shape of this end, the highest magnetic field could be shifted and averaged. The SLAC mushroom cavity [26, 27] uses TE_{013} like mode at 11.4 GHz with 2 inch diameter sample. Three TE_{011} modes have been stacked together and the top plate has been reshaped to a mushroom structure, so that the magnetic field could be averaged on a larger surface area. The peak magnetic field on the sample is 2.5 times of the peak magnetic field on the cavity wall. The SLAC mushroom cavity is constructed out of copper so that pulsed RF power could be conducted into the cavity and the loaded Q will not degrade that much until the sample reaches its critical field. The Q of this Cu cavity with a Cu sample is measured to be 50,000 at room temperature and 224,000 at 4K. The Q of this Cu cavity with a superconducting sample is measured to be 342,000. The drawback of using a copper cavity is that the Q of the whole setup is mainly determined by the copper cavity, and is less sensitive to the contribution from the superconducting sample. The precision of the surface resistance measurement is estimated to be up to 0.1 m Ω . The maximum magnetic field that can be reached in the current system is up to 300-400 mT, it is excellent for precise measurement of the quenching magnetic field of the superconducting samples. Recently a Cu mushroom cavity with Nb coating was fabricated and commissioned at SLAC. The Q of this Nb cavity, with a single crystal bulk Nb reference sample that is assumed to have the same surface resistance as the cavity, is around 2×10^7 , with helium bath temperature at 4 K. The surface resistance of the reference sample is estimated to be 65 $\mu\Omega$. [59]

The Cornell mushroom cavity [41, 44], with cavity geometry similar to the SLAC version, is a niobium cavity that provides higher measurement resolution. The peak magnetic field on the sample is 1.57 times greater than the peak magnetic field on the cavity wall for the TE_{013} like mode at 6.16 GHz, and 1.24 times greater for the TE_{012} like mode at 4.78 GHz, with sample diameter of 4 inches. A third generation of this cavity resonates at 3.9 GHz and reaches a peak field over 100 mT on the sample surface and an unloaded cavity Q_0 over 10^{10} . Recently this cavity has been used to measure the surface resistance of samples produced by High Power Impulse Magnetron Scattering (HiPIMS) [60].

Another mushroom cavity is designed at TAMU [42, 61]. The sample size of this cavity is 7 inch in diameter. Sapphire is inserted into the mushroom cavity to reduce the resonance frequency of the TE_{01} mode to 2.2 GHz. In this model, the maximum surface magnetic field in the cavity is 9.02 times higher than the field anywhere else in the cavity. This cavity is shown in Figure below [42].



366

367

368

369

370

371

372

373

374

375

376

377

378

379

380

381

382

383

384

385

386

387

388

389

390

391

392

Figure 4: The Wafer Test Cavity. In the center, the sapphire is hung slightly above the surface of the sample located at the bottom. The sample (not shown in this figure) is held by a mating bottom flange containing an array of CernoxTM resistor thermometry. The sapphire extends beyond the cavity for cooling and as a means of mechanical stabilization. Two side ports are located on upper part of the cavity to provide power, insert diagnostic tools such as a probe antenna, and vacuum port. [42]

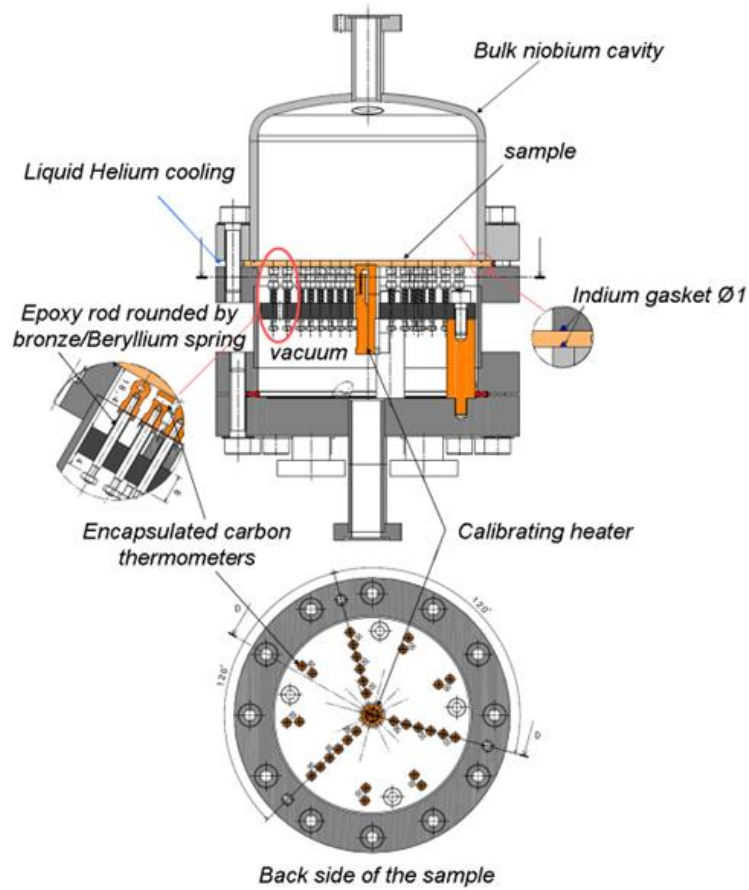
The SLAC mushroom cavity has been used to measure the surface resistance and the RF quench field of Nb and MgB₂[27]. The Cornell mushroom cavity, and its alternative, sample host cavity, is used to measure bulk Nb and thin film Nb up to 106 mT, and it is planned to be used in investigating thin-film materials such as NbN on MgO, thin-film Nb, Nb on Cu on Nb, and MgB₂[41, 44, 60].

3.4. Orsay cavity

A cylindrical TE₀₁₁/TE₀₁₂ cavity enabling measurements at 4 and 5.6GHz has been developed in collaboration between CEA Saclay and IPN Orsay [22, 62] to test the surface resistance of superconducting Nb and NbTiN thin films sputtered on removable copper disks. The goal was to develop a system with improved accuracy, especially at 4 K, compared to a cylindrical niobium cavity, which used the end-plate replacement technique, relying on a reference sample. It gave a resolution of about ± 1000 n Ω at 4K. The developed calorimetric system consists of a cylindrical cavity and a thermometric part. The thermometric part is located in a vacuum insulation jacket, where a dismountable assembly with a static heater and 24 thermometers is installed, see Figure [62].

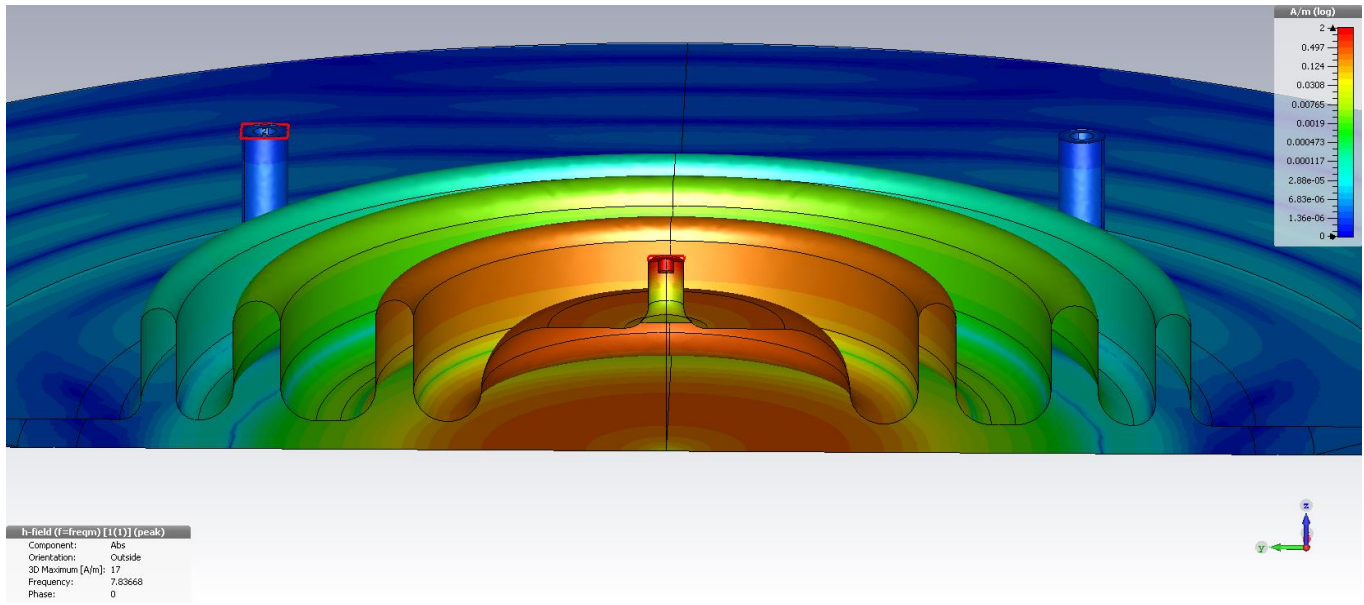
The cavity has been used for systematic studies of the surface resistance of sputtered niobium on copper samples. Substrates of different roughness have been investigated. A correlation between surface roughness and surface resistance could be made, see reference [22]. The residual resistance of the thin film samples was found to scale linear with frequency [22]. More recently a slightly modified cavity based on the same geometry has been developed for further thin film studies [30]. This cavity has been used to measure the

393 surface resistance of a sample comprised of nanometer thin alternating superconducting and insulating lay-
 394 ers for the first time [63]. For a low surface magnetic field of 1 mT and temperatures above 3 K the surface
 395 resistance of the multilayered sample was found to be significantly lower than for a niobium reference
 396 sample.



397
 398 Figure 5: Set-up of the TE_{011}/TE_{012} cavity. Reproduced with the permission of G. Martinet.

399
 400 3.5. Choked resonator
 401



402
403 Figure 6: Simulated magnetic field intensity distribution on the cavity (top) and sample (bottom) surfaces.

404
405 A system currently in development is the Choked Resonator. It is designed to allow fast sample changes
406 while not compromising performance and accuracy. The design called for a simple system able to measure
407 flat sample surfaces without requiring complex assembly procedures or having to worry about the quality
408 of the join between sample and cavity.

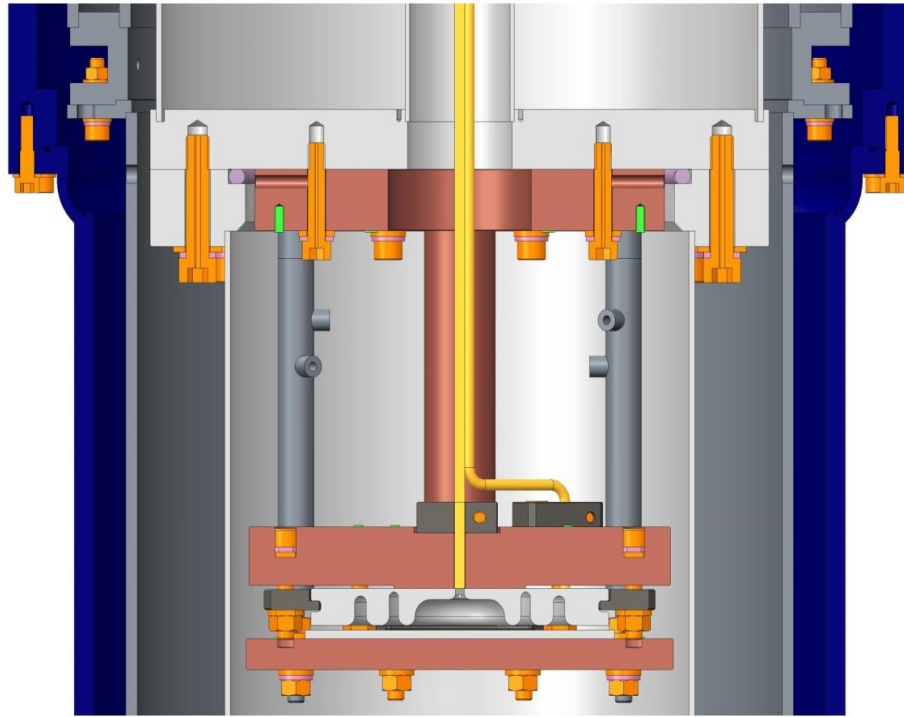
409
410 It operates in a TM_{010} -like mode (see Figure 6) and consists of two parts:

- 411 • A bulk niobium resonator, surrounded by RF chokes optimized to minimize the leakage field.
412 The RF input coupler is located in this piece. The input coupler is rigidly attached to a rod linked to
413 a micrometer so as to adjust its penetration into the cavity.
- 414 • A flat sample piece, which is the part to be studied, is separated from the cavity body with a
415 vacuum gap of ~ 2.5 mm. An RF probe can be inserted in the gap to provide transmission measure-
416 ments.

417 Simulations show that 37% of the RF-induced heating will occur on the sample plate, the remainder
418 being on the cavity (assuming identical materials). The peak magnetic field is located on the sample plate
419 and thus the maximum measurable breakdown field exceeds that of bulk niobium.

420 The resonator is supported in a cradle placed in a vacuum volume as shown in Figure 7. The cradle is
421 designed so that the two parts of the resonator are thermally isolated from one another. The cavity is
422 mounted onto a support plate strongly connected to the helium tank, while the sample is mounted onto a
423 separate plate supported by a much weaker thermal link. This allows direct measurement of RF losses in
424 the sample using the calorimetric technique described above.

425 The sample can be changed easily by removing the sample holder and swapping it with another,
426 mounted with a new sample to study. All that needs to be done is to reattach three supporting double-nuts
427 and reconnect the heater and thermometry cables before the vacuum chamber shield can be sealed again.



Clipping State:1.0

428

429

430

431

432

433

434

435

436

437

438

439

440

441

442

443

444

445

446

447

448

449

450

451

Figure 7: Choked resonator in its cradle (in this case, a 2-choked prototype is depicted). The cavity is connected to the helium bath by a solid copper pillar which provides a strong thermal link to the LHe bath. The sample plate is mounted on a copper plate supported by thin-walled stainless steel pillars which provide a weak thermal link to the LHe bath. The cradle sits in the inner vacuum chamber which is separate from the outer vacuum chamber which provides thermal insulation.

The current choked resonator is a 7.8 GHz design, due to the maximum size of the samples that can be deposited using the equipment available at Daresbury. This allows the testing of sample pieces from 5 cm to 10 cm diameter. The concept can easily be scaled to other frequencies, given a large enough vacuum vessel.

A full cryogenic test hasn't been carried out at time of writing, but is expected to validate the design soon.

4. Summary

In this article we have reviewed devices to characterize SRF materials. These systems have basically two advantages compared to cavity tests. The first one is that small flat samples can be tested. This allowed for example to obtain the surface resistance of MgB_2 with the SIC and of a multilayered sample using the $\text{TE}_{011}/\text{TE}_{012}$ cavity. Neither material is yet sufficiently technologically advanced to be deposited on the inner surface of a cavity. The other advantage is that with a sample test cavity one is not constrained by the field geometry required in an accelerating cavity. This is used in the Quadrupole Resonators with its several resonant modes at different frequencies and almost identical field magnetic configuration. Such a device is therefore ideally suited to test theoretical surface resistance models.

452 In general the goal for the design of a test cavity is to have a low resonance frequency f_0 , a high magnetic
 453 field B_{\max} on the sample, a high ratio of sample to cavity magnetic field $B_{\max \text{ sample}}/B_{\max \text{ cavity}}$ and a high
 454 sensitivity. Rate of sample throughput is also important, given the number of samples to test that any opti-
 455 mization process generates. This poses challenging and conflicting design constraints. Some devices cur-
 456 rently in use or under development are compared to each other with respect to these parameters in Table 1.
 457 Using the Quadrupole Resonators from CERN or HZB it is possible to obtain R_s at multiple frequencies of
 458 interest concerning accelerator application over a temperature range inaccessible to standard cavity meas-
 459 urements. The disadvantage of this device is its more complicated sample changing procedure, requiring
 460 electron beam welding of a flat sample disk to the sample cylinder. The SIC system is capable of measuring
 461 flat samples with high resolution but at higher frequency and lower magnetic field. The Quadrupole Reso-
 462 nators, SIC, Orsay cavity and the Choked Cavity rely on the calorimetric technique to achieve their high
 463 resolution. The drawback of this approach is again the more complicated design, since it requires the ther-
 464 mal decoupling of the sample from the host cavity. The Cornell mushroom cavity relying on T-mapping
 465 can give a good resolution with a less complicated design. It is however more difficult to derive the absolute
 466 value of the surface resistance by this approach. An unmatched maximum field on the sample surface is
 467 obtained by the SLAC mushroom cavity. Being made of copper this device has a poor sensitivity making
 468 it a more suitable tool for critical field measurements. In summary all devices reviewed in the article can
 469 give valuable insights into loss mechanisms under RF and allow the testing of new materials for SRF ap-
 470 plications. Each of them has unique features, advantages and disadvantages compared to the others depend-
 471 ing on application.

472
 473 Table 1: Comparison of the different devices and alternative devices.

Device	Frequency [GHz]	Sample diameter [mm]	Sensitivity	B_{\max} [mT]	$B_{\max \text{ sample}}/B_{\max \text{ cavity}}$
SIC	7.4	50	Sub $n\Omega$	14	1.04
Quadrupole Resonator (CERN)	0.4/0.8/1.2	75	Sub $n\Omega$	70	1.18
Quadrupole Resonator (HZB)	0.433/0.866/1.3	75	Sub $n\Omega$	120	0.89
Orsay	4/5.6	126	Few $n\Omega$	16	
SLAC mushroom	11.4	50	0.1 $m\Omega$ Cu cavity /10 $\mu\Omega$ Nb cavity	400	2.5
Cornell mushroom	4.78/6.16	100		106	1.24/1.57
TAMU sapphire-loaded	2.2	178			9.02
Choked resonator	7.8	100	Few $n\Omega$ (est.)	10 (@4.2K)	1.18

474

475 5. Outlook

476

477 The future of SRF cavity development most likely resides in coatings to improve on cavity properties. A
 478 substantial research effort is taking place in that field. However, in order to validate coating methods and

inform their optimization there is a need for a reliable, affordable and informative method of testing the SRF properties of thin film materials. Alternative methods to cavity measurements exist, but they can only reveal part of the picture. It is therefore essential to be able to perform measurements of samples in SRF conditions.

The ideal sample test cavity would have a high resolution only obtainable by the calorimetric approach, could accommodate small samples of about 2 cm diameter, have a resonance frequency below 3 GHz and a maximum field close to the superheating field of niobium. A small sample size is a key aspect to provide convenient portability between the RF system, the deposition system and surface analysis tools. Experience has shown that a high turnaround not only requires a fairly simple design but also dedicated staff and test environment. The cavities that have been developed so far each offer only a partial solution to that need. Quadrupole resonators, for instance, provide extremely high-sensitivity measurements over a wide parameter range, but are rather time-consuming to reset for a new sample. This type of instrument is suitable for experiments aimed at increasing the understanding of the behavior of thin films on a fundamental level but far less suited to sample swapping repeatedly.

It is however apparent from the backlog of untested samples developed by various teams across the community that a cavity that can be used with a fast turn-around time is essential to allow the sorting of promising samples from less performing ones. The choked resonator when successfully commissioned could fulfill the need for fast turnaround and high precision but still has the drawback of a relatively large sample size and high resonant frequency. Further developments should aim to overcome these limitations. This cavity would also ideally allow operation at high fields and be a dedicated system with sufficient resource to keep the sample testing rate optimal. Should compromises need to be made, it would be advisable to aim for high turnover and medium precision.

Acknowledgment

This work is supported by Jefferson Science Associates, LLC under U.S. DOE Contract No. DE-AC05-06OR23177, by DOE under Contract No. DE-SC0004410, by Brookhaven Science Associates, LLC under US DOE contract No. DE-AC02-98CH10886, and by a Marie Curie International Outgoing Fellowship within the EU Seventh Framework Programme for Research and Technological Development (2007-2013). One of us (TJ) is indebted to the German Ministry of Education and Research for being awarded a grant by the German Doctoral Program at CERN (Gentner - Program). This work was also supported by the UK Science & Technology Facility Council (STFC). The authors would like to thank Lewis Gurrán for his insights into the manuscript.

References

- [1] Poole C P, Farach H A and Creswick R J 1999 Handbook of Superconductivity. (London: Academic Press)
- [2] Benvenuti C, Circelli N and Hauer M 1984 Niobium Films for Superconducting Accelerating Cavities *Appl. Phys. Lett.* **45** 583-4
- [3] Padamsee H, Knobloch J and Hays T 1998 *RF Superconductivity for Accelerators* (Weinheim, Germany: Wiley-VCH)
- [4] Geng R L, Ereemeev G V, Padamsee H and Shemelin V D 2007 High Gradient Studies for ILC With Single-Cell Re-Entrant Shape and Elliptical Shape Cavities Made of Fine-Grain and Large-Grain Niobium. In: *Proceedings of the 2007 Particle Accelerator Conference*, (Albuquerque, New Mexico) p 2337

- 526 [5] Palmieri V 2001 New Materials for Superconducting Radiofrequency Cavities. In: *Proceedings of*
527 *the 10th Workshop on RF Superconductivity*, (Tsukuba, Japan) p 162
- 528 [6] Posen S, Liepe M and Hall D L 2015 Proof-of-principle demonstration of Nb₃Sn superconducting
529 radiofrequency cavities for high Q₀ applications *Appl. Phys. Lett.* **106** 082601
- 530 [7] Posen S, Valles N and Liepe M 2015 Radio Frequency Magnetic Field Limits of Nb and Nb₃Sn
531 *Physical Review Letters* **115** 047001
- 532 [8] Gurevich A 2006 Enhancement of RF Breakdown Field of Superconductors by Multilayer Coating
533 *Appl. Phys. Lett.* **88** 012511
- 534 [9] James C, Krishnan M, Bures B, Tajima T, Civale L, Edwards R, Spradlin J and Inoue H 2013
535 Superconducting Nb Thin Films on Cu for Applications in SRF Accelerators *IEEE*
536 *TRANSACTIONS ON APPLIED SUPERCONDUCTIVITY* **23** 3500205
- 537 [10] Leviev G I, Genkin V M, Tsindlekht M I, Felner I, Paderno Y B and Filippov V B 2005 Low-
538 Frequency Response in the Surface Superconducting State of Single-Crystal ZrB₁₂ *Phys. Rev. B* **71**
539 064506
- 540 [11] Bahte M, Herrmann F and Schmäser P 1997 Magnetization and Susceptibility Measurements on
541 Niobium Samples for Cavity Production. In: *Proceedings of the 1997 Workshop on RF*
542 *Superconductivity*, (Abano Terme, Padova, Italy) p 881
- 543 [12] Malyshev O B, Gurran L, Pattalwar S, Pattalwar N, Dumbell K D, Valizadeh R and Gurevich A
544 2015 A Facility for Magnetic Field Penetration Measurements on Multilayer S-I-S Structures. In:
545 *Proceedings of the 17th International Conference on RF Superconductivity*, (Whistler, Canada) p
546 716
- 547 [13] Antoine C 2012 Materials and surface aspects in the development of SRF Niobium cavities
548 *EuCARD Work Package 10: SC RF technology for higher intensity proton accelerators and higher*
549 *energy electron linacs, Editorial Series on Accelerator Science*
- 550 [14] Ciovati G, Anlage S M, Baldwin C, Cheng G, Flood R, Jordan K, Kneisel P, Morrone M, Nemes G,
551 Turlington L, Wang H, Wilson K and Zhang S 2012 Low Temperature Laser Scanning Microscopy
552 of a Superconducting Radio-Frequency Cavity *Review of Scientific Instruments* **83** 034704
- 553 [15] Gurevich A and Ciovati G 2013 Effect of Vortex Hotspots on the Radio-Frequency Surface
554 Resistance of Superconductors *Phys. Rev. B* **87** 054502
- 555 [16] Badan L, Durand C, Palmieri V, Preciso R, Stark S, Stivanello F and Venturini W 1998 RF
556 Characterization of Small Scale Cavities *Particle Accelerators* **62** 117-23
- 557 [17] Palmieri V, Antonio Alessandro R, Sergey Yu S and Ruggero V 2014 Evidence for Thermal
558 Boundary Resistance Effects on Superconducting Radiofrequency Cavity Performances *Supercond.*
559 *Sci. Technol.* **27** 085004
- 560 [18] Yao Z 2015 Medium Field Q-Slope in Low β Resonators. In: *Proceedings of the 17th International*
561 *Conference on RF Superconductivity*, (Whistler, Canada)
- 562 [19] Tai T, Ghamsari B G, Bieler T R, Tan T, Xi X X and Anlage S M 2014 Near-Field Microwave
563 Magnetic Nanoscopy of Superconducting Radio Frequency Cavity Materials *Appl. Phys. Lett.* **104**
564 232603
- 565 [20] Delayen J R, Bohn C L and Roche C T 1990 Measurements of the Surface Resistance of High-T_c
566 Superconductors at High RF Fields *Journal of Superconductivity* **3** 243-50
- 567 [21] Allen L H 1986 The Surface Resistance of Superconducting A15 Niobium-Tin Films at 8.6 GHz.
568 In: *Department of Physics*, (Standord, California: Stanford University)
- 569 [22] Fouaidy M, Bosland P, Ribeauudeau M, Chel S and Juillard M 2002 New Results on RF Properties
570 of Superconducting Niobium Films Using a Thermometric System. In: *Proceedings of the 8th*
571 *European Particle Accelerator Conference*, (Paris, France: EPS-IGA and CERN) pp 2229-31

- 572 [23] Tonkin B A and Proykova Y G 1993 Modular System for Microwave Surface Impedance
573 Measurement of High Temperature Superconductors *Supercond. Sci. Technol.* **6** 7
- 574 [24] Liang C 1993 A New Surface Resistance Measurement Method with Ultrahigh Sensitivity. In:
575 *Physics*, (Blacksburg, Virginia: Virginia Polytechnic Institute and State University)
- 576 [25] Kneisel P, Muller G and Reece C 1987 Investigation of the Surface Resistance of Superconducting
577 Niobium Using Thermometry in Superfluid Helium *IEEE Transactions on Magnetics* **MAG-23**
578 1417-21
- 579 [26] Nantista C, Tantawi S, Weisend J, Siemann R, Dolgashev V and Campisi I 2005 Test Bed for
580 Superconducting Materials. In: *Proceedings of the 2005 Particle Accelerator Conference*,
581 (Knoxville, TN) pp 4227-9
- 582 [27] Guo J, Tantawi S, Martin D and Yoneda C 2011 Cryogenic RF Material Testing with a High-Q
583 Copper Cavity. In: *Advanced Accelerator Concepts: 14th Workshop*, ed S H Gold and G S
584 Nusinovich p 330
- 585 [28] Klein N, Muller G, Piel H, Roas B, Schultz L, Klein U and Peiniger M 1988 Millimeter Wave
586 Surface Resistance of Epitaxially Grown $\text{YBa}_2\text{Cu}_3\text{O}_{7-x}$ Thin Films *Applied Physics Letter* **54** 3
- 587 [29] Misra M, Kataria N D and Srivastava G P 2000 Laterally Resolved Microwave Surface-Resistance
588 Measurement of High- T_c Superconductor Samples by Cavity Substitution Technique *IEEE*
589 *Transactions on Microwave Theory and Techniques* **48** 791-801
- 590 [30] Martinet G, Blivet S, Hammoudi N and Fouaidy M 2009 Development of a TE_{011} Cavity for Thin-
591 Films Study. In: *Proceedings of the 14th International Conference on RF Superconductivity*,
592 (Berlin-Dresden, Germany) pp 293-6
- 593 [31] Phillips L, Davis G K, Delayen J R, Ozelis J P, Plawski T, Wang H and Wu G 2005 A Sapphire
594 Loaded TE_{011} Cavity for Superconducting Impedance Measurements - Design, Construction and
595 Commissioning Status. In: *Proceedings of the 12th International Workshop on RF*
596 *Superconductivity*, (Ithaca, NY) pp 349-51
- 597 [32] Xiao B P, Reece C E, Phillips H L, Geng R L, Wang H, Marhauser F and Kelley M J 2011 Radio
598 Frequency Surface Impedance Characterization System for Superconducting Samples at 7.5 GHz
599 *Review of Scientific Instruments* **82** 056104
- 600 [33] Xiao B P 2012 Surface Impedance of Superconducting Radio Frequency Materials. In: *Department*
601 *of Applied Science: The College of William and Mary*
- 602 [34] Xiao B P, Reece C E, Phillips H L and Kelley M J 2012 Calorimeters for Precision Power
603 Dissipation Measurements on Controlled-Temperature Superconducting Radiofrequency Samples
604 *Review of Scientific Instruments* **83** 124905
- 605 [35] Mahner E, Calatroni S, Chiaveri E, Haebel E and Tessier J M 2003 A New Instrument to Measure
606 the Surface Resistance of Superconducting Samples at 400 MHz *Review of Scientific Instruments*
607 **74** 3390-4
- 608 [36] Junginger T, Weingarten W and Welsch C 2009 RF Characterization of Superconducting Sample.
609 In: *Proceedings of the 14th International Conference on RF Superconductivity*, (Berlin-Dresden,
610 Germany) pp 130-6
- 611 [37] Rubin D L, Green K, Gruschus J, Kirchgessner J, Moffat D, Padamsee H, Sears J, Shu Q S,
612 Schneemeyer L F and Waszczak J V 1988 Observation of a Narrow Superconducting Transition at
613 6GHz in Crystals of YBCO *Phys. Rev. B* **38** 6538-42
- 614 [38] Ormeno R J, Morgan D C, Broun D M, Lee S F and Waldram J R 1997 Sapphire Resonator for the
615 Measurement of Surface Impedance of High-Temperature Superconducting Thin Films *Review of*
616 *Scientific Instruments* **68** 2121-6

- 617 [39] Bruynseraede Y, Gorle D, Leroy D and Morignot P 1971 Surface-Resistance Measurements in
618 TE₀₁₁-Mode Cavities of Superconducting Indium, Lead and an Indium-Lead Alloy at Low and High
619 RF Magnetic Fields *Physica* **54** 137-59
- 620 [40] Junginger T 2012 Investigations of the Surface Resistance of Superconducting Materials. In:
621 *Combined Faculties for the Natural Sciences and for Mathematics*, (Heidelberg, Germany: Ruperto-
622 Carola University)
- 623 [41] Xie Y 2013 Development of Superconducting RF Sample Host Cavities and Study of Pit-Induced
624 Cavity Quench. In: *Department of Physics*, (Ithaca, NY: Cornell University)
- 625 [42] Comeaux J K 2014 Testing and Simulation of the SRF Wafer Test Cavity for the Characterization
626 of Superconductors and Heterostructures. In: *Department of Physics and Astronomy*, (College
627 Station, Texas: Texas A&M University)
- 628 [43] Kleindienst R, Burrill A, Keckert S, Knobloch J and Kugeler O 2015 Commissioning Results of the
629 HZB Quadrupole Resonator. In: *Proceedings of the 17th International Conference on RF*
630 *Superconductivity*, (Whistler, Canada) p 930
- 631 [44] Maniscalco J T, Clasby B, Gruber T, Hall D L and Liepe M 2015 Recent Results from the Cornell
632 Sample Host Cavity. In: *Proceedings of the 17th International Conference on RF Superconductivity*,
633 (Whistler, Canada) p 626
- 634 [45] Dhakal P, Ciovati G and Myneni G R 2012 A Path to Higher Q₀ with large grain Niobium cavities.
635 In: *International Particle Accelerator Conference 2012*, (New Orleans, Louisiana, USA)
- 636 [46] Dhakal P, Ciovati G, Myneni G R, Gray K E, Groll N, Maheshwari P, McRae D M, Pike R, Proslie
637 T, Stevie F, Walsh R P, Yang Q and Zasadzinski J 2013 Effect of High Temperature Heat
638 Treatments on the Quality Factor of a Large-Grain Superconducting Radio-Frequency Niobium
639 Cavity *Phys. Rev. Spec. Top. Accel Beams* **16** 042001
- 640 [47] Grassellino A, Romanenko A, Sergatskov D, Melnychuk O, Trenikhina Y, Crawford A, Rowe A,
641 Wong M, Khabiboulline T and Barkov F 2013 Nitrogen and Argon Doping of Niobium for
642 Superconducting Radio Frequency Cavities: A Pathway to Highly Efficient Accelerating Structures
643 *Supercond. Sci. Technol.* **26** 102001
- 644 [48] Xiao B P, Geng R L, Kelley M J, Marhauser F, Phillips H L, Reece C E and Wang H 2009 RF
645 Surface Impedance Measurement of Polycrystalline and Large Grain Nb Disk Sample at 7.5 GHz.
646 In: *Proceedings of the 14th International Conference on RF Superconductivity*, (Berlin-Dresden,
647 Germany) p 305
- 648 [49] Xiao B P, Geng R L, Kelley M J, Marhauser F, Phillips H L, Reece C E and Wang H 2009
649 Commissioning of the SRF Surface Impedance Characterization System at Jefferson Lab. In:
650 *Proceedings of the 23rd Particle Accelerator Conference*, (Vancouver, Canada) p 2144
- 651 [50] Xiao B P, Zhao X, Spradlin J, Reece C E, Kelley M J, Tan T and Xi X X 2012 Surface Impedance
652 Measurements of Single Crystal MgB₂ Films for Radiofrequency Superconductivity Applications
653 *Supercond. Sci. Technol.* **25** 095006
- 654 [51] Xiao B P, Ereemeev G V, Kelley M J, Phillips H L and Reece C E 2012 RF Surface Impedance
655 Characterization of Potential New Materials for SRF-Based Accelerators. In: *Proceedings of XXVI*
656 *Linear Accelerator Conference*, (Tel Aviv, Israel) p 312
- 657 [52] Lukaszew R A, Beringer D B, Roach W M, Ereemeev G V, Reece C E, Valente-Feliciano A-M and
658 Xi X 2013 Proof of Concept Thin Films and Multilayers toward Enhanced Field Gradients in SRF
659 Cavities. In: *Proceedings of 16th International Conference on RF Superconductivity*, (Cite
660 Internationale Universitaire, Paris, France) p 782
- 661 [53] Ereemeev G, Phillips L, Reece C E, Valente-Feliciano A-M and Xiao B P 2013 Characterization of
662 Superconducting Samples with SIC System for Thin Film Developments: Status and Recent Results.

- 663 In: *Proceedings of 16th International Conference on RF Superconductivity*, (Cite Internationale
664 Universitaire, Paris, France) p 599
- 665 [54] Sosa-Guitron S, Gurevich A, Delayen J R, Ereemeev G, Sundhal C and C.-B.Eom 2015
666 Measurements of RF Properties of Thin Film Nb₃Sn Superconducting Multilayers using a
667 Calorimetric Technique. In: *Proceedings of the 17th International Conference on RF
668 Superconductivity*, (Whistler, Canada) p 720
- 669 [55] Junginger T, Weingarten W and Welsch C 2012 Extension of the Measurement Capabilities of the
670 Quadrupole Resonator *Review of Scientific Instruments* **83** 063902
- 671 [56] Aull S, Junginger T, Sublet A, Delsolaro W V, Zhang P, Valente-Feliciano A-M and Knobloch J
672 2015 On the Understanding of Q-Slope of Niobium Thin Films. In: *Proceedings of the 17th
673 International Conference on RF Superconductivity*, (Whistler, Canada) p 494
- 674 [57] Kleindienst R, Kugeler O and Knobloch J 2013 Development of an Optimized Quadrupole
675 Resonator at HZB. In: *Proceedings of 16th International Conference on RF Superconductivity*, (Cite
676 Internationale Universitaire, Paris, France) p 614
- 677 [58] Keckert S, Kleindienst R, Knobloch J and Kugeler O 2015 Design and First Measurements of an
678 Alternative Calorimetry Chamber for the HZB Quadrupole Resonator. In: *Proceedings of the 17th
679 International Conference on RF Superconductivity*, (Whistler, Canada) p 739
- 680 [59] Welander P, Tantawi S and Franzi M 2016 A Test Cavity & Cryostat for Rapid RF Characterization
681 of Superconducting Materials. In: *7th International Workshop on Thin Films and New Ideas for
682 Pushing the Limits of RF Superconductivity*, (Jefferson Lab, Virginia, USA)
- 683 [60] Maniscalco J T, Hall D L, Liepe M, Malyshev O B, Valizadeh R and Wilde S 2016 New Material
684 Studies in the Cornell Sample Host Cavity. In: *Proceedings of the 7th International Particle
685 Accelerator Conference*, (BEXCO, Busan Korea)
- 686 [61] Pogue N J, McIntyre P M, Sattarov A I and Reece C 2011 Ultra-Gradient Test Cavity for Testing
687 SRF Wafer Samples *IEEE TRANSACTIONS ON APPLIED SUPERCONDUCTIVITY* **21** 1903-7
- 688 [62] Ribeau deau M, Charrier J P, Chel S, Juillard M, Fouaidy M and Caruette M 1998 RF Surface
689 Resistance Measurements of Superconducting Samples with Vacuum Insulated Thermometers. In:
690 *Proceedings of the 6th European Particle Accelerator Conference*, (Stockholm, Sweden)
- 691 [63] Antoine C Z, Villegier J-C and Martinet G 2013 Study of Nanometric Superconducting Multilayers
692 for RF Field Screening Applications *Appl. Phys. Lett.* **102** 102603
- 693
- 694